REPORT DOCUMENTATION PAGE

Form Approved
OMB No 0704-0188

AD-A270 780

REPORT DATE	3. REPORT TYPE AND DATES COVERED
1993	Open literature publication

4. TITLE AND SUBTITLE
Comparative morphology of sulfur mustard effects in the hairless guinea pig and a human skin equivalent

5. FUNDING NUMBERS
62787A 3M162787A875 AA

6. AUTHOR(S)
Petrali, JP, Oglesby, SB, Hamilton, TA, Mills, KR

7. PERFORMING ORGANIZATION NAME(S) AND ADDRESS(ES)
US Army Medical Research Institute of Chemical Defense
ATTN: SGRD-UV- YC
Aberdeen Proving Ground, MD 21010-5425

8. PERFORMING ORGANIZATION REPORT NUMBER

9. SPONSORING/MONITORING AGENCY NAME(S) AND ADDRESS(ES)
USAMRICD
ATTN: SGRD-UV-RC
APG, MD 21010-5425

10. SPONSORING/MONITORING AGENCY REPORT NUMBER
USAMRICD-P91-053

11. SUPPLEMENTARY NOTES
Appeared in Journal of Submicroscopic Cytol. Pathol., 25(1), 113-118, 1993

12a. DISTRIBUTION/AVAILABILITY STATEMENT
Approved for public release; distribution unlimited

12b. DISTRIBUTION CODE

13. ABSTRACT *(Maximum 200 words)*

SUMMARY - A commercially available human skin equivalent (HSE) was used as an *in vitro* organotypic skin model to study temporal morphological effects of sulfur mustard gas (HD). Light and electron microscopic analyses of the HD-human skin equivalent model (HD-HSE) were compared to the HD-hairless guinea pig model (HD-HGP). HSE samples were exposed to 10 µl HD vapor for 8 min and harvested at selected times up to 24 h. Skin sites of HGP were exposed to the same vapor dose or to 2.0 µl liquid HD for 30 min and collected at 12 and 24 h. In both models, basal cells of the stratum germinativum were selectively affected. The HD-HSE study revealed that basal cell changes began 3 to 6 h following exposure. These early cellular changes included an acanthолysis of some basal cells with widening of intercellular spaces, disruption of desmosomal attachments, nuclear pyknosis, perinuclear blebbing and repositioning of cytoplasmic tonofilaments to a perinuclear position. At 12 to 24 h, basal cell pathology progressed to diffuse swelling of endoplasmic reticula, cytoplasmic vacuolations and necrosis which now extended to supra basal cell layers. Comparing basement membrane zone effects, HD-HGP consistently developed characteristic microblisters at the dermal-epidermal junction; however, HD-HSE with its absence of a morphologically distinguishable basement membrane did not. Instead, cellular fragments, granules and debris accumulated early in this area to thicken regions usually assigned to the lamina lucida and lamina densa of a true basement membrane leading to complete separation of dermis from epidermis at later time periods.

14. SUBJECT TERMS
sulfur mustard, human skin equivalent, ultrastructure, hairless guinea pig, basement membrane zone

15. NUMBER OF PAGES
6

16. PRICE CODE

17. SECURITY CLASSIFICATION OF REPORT	18. SECURITY CLASSIFICATION OF THIS PAGE	19. SECURITY CLASSIFICATION OF ABSTRACT	20. LIMITATION OF ABSTRACT
UNCLASSIFIED	UNCLASSIFIED	UNCLASSIFIED	None

J. SUBMICROSC. CYTOL. PATHOL., 25 (1), 113-118, 1993

Comparative morphology of sulfur mustard effects in the hairless guinea pig and a human skin equivalent

J.P. PETRALI, S.B. OGLESBY, T.A. HAMILTON and K.R. MILLS

Comparative Pathology, United States Army Medical Research Institute of Chemical Defense, Aberdeen, Maryland, USA

SUMMARY - A commercially available human skin equivalent (HSE) was used as an *in vitro* organotypic skin model to study temporal morphological effects of sulfur mustard gas (HD). Light and electron microscopic analyses of the HD-human skin equivalent model (HD-HSE) were compared to the HD-hairless guinea pig model (HD-HGP). HSE samples were exposed to 10 µl HD vapor for 8 min and harvested at selected times up to 24 h. Skin sites of HGP were exposed to the same vapor dose or to 2.0 µl liquid HD for 30 min and collected at 12 and 24 h. In both models, basal cells of the stratum germinativum were selectively affected. The HD-HSE study revealed that basal cell changes began 3 to 6 h following exposure. These early cellular changes included an acantholysis of some basal cells with widening of intercellular spaces, disruption of desmosomal attachments, nuclear pyknosis, perinuclear blebbing and repositioning of cytoplasmic tonofilaments to a perinuclear position. At 12 to 24 h, basal cell pathology progressed to diffuse swelling of endoplasmic reticula, cytoplasmic vacuolations and necrosis which now extended to supra basal cell layers. Comparing basement membrane zone effects, HD-HGP consistently developed characteristic microblisters at the dermal-epidermal junction; however, HD-HSE with its absence of a morphologically distinguishable basement membrane did not. Instead, cellular fragments, granules and debris accumulated early in this area to thicken regions usually assigned to the lamina lucida and lamina densa of a true basement membrane leading to complete separation of dermis from epidermis at later time periods.

KEY WORDS *sulfur mustard - human skin equivalent - ultrastructure - hairless guinea pig - basement membrane zone*

INTRODUCTION

We have previously reported morphological correlates of sulfur mustard (HD) toxicity in several model systems: the human skin grafted athymic nude mouse (Papirmeister *et al.*, 1984) the hairless guinea pig, and human cells in culture (Petrali *et al.*, 1990). We are now documenting HD effects in a human skin equivalent model, Testskin® (Petrali *et al.*, 1991), and comparing these effects with those of the hairless guinea pig (HGP) as well as those already reported for other animal model systems and isolated human cells in culture. The human skin equivalent (HSE) is an *in vitro* differentiated stratified cellular system composed of a well organized epidermis and dermis which is finding increasing research use in skin toxicity and related studies (Bell *et al.*, 1989). It is investigated here expressly as an organotypic skin model to bridge experimental knowledge gaps between HD effects in animal models and human monotypic cells in culture. Additionally, it is allowing for study of HD toxicity which circumvents concern of using human extracted skin tissue for a human response and lessens dependence on animal models for similar studies. This study summarizes and compares HD effects in the HSE and the HGP with anticipation that disclosing morphological correlates of HD toxicity in differing model systems will generate a useful morphologic data base against which prophylactic and therapeutic regimens might be measured.

Mailing address: Dr. John P. Petrali, Comparative Pathology, USAMRICD, APG, Maryland, 21010-5425, USA.

MATERIALS AND METHODS

HD-HSE

A human skin equivalent obtained as living skin equivalent testwell kits from Organogenesis, Inc., Cambridge, MA., was exposed by vapor cup (Mershon *et al.*, 1990) to 10 μl HD for 8 min at room temperature, replenished with maintenance medium (Organogenesis, Inc.) incubated at 37 °C in an atmosphere of 5% carbon dioxide and harvested at 1, 3, 6, 12 and 24 h following exposure. Control samples not exposed to HD but having undergone similar experimental handling were collected at 0 and 24 h.

HD-HGP

Skin sites of hairless guinea pigs were exposed to either 10 μl HD vapor for 8 min or 2 μl liquid HD for 30 min with the animal under sedation with Ketamine HCL (0.3 mg/kg I.M.) and Rompun (0.3 mg/kg I.M.). Unexposed semiadjacent skin sites were used as controls. Following exposure, animals were anesthesized with sodium pentobarbitol (26.8 mg/kg I.P.) and skin sites harvested at selected time periods up to 24 h. After extraction of skin sites, animals were euthanatized by exsanguination through the abdominal aorta. For purposes of this report, postexposure time periods available for comparison to the HD-HSE study were 12 and 24 h. HD used for exposures was from Lot # HD-U-4244-CTF-N-1, 97.9% purity, USAMRICD, APG, MD.

Tissue processing

HD-exposed and control samples were immersion fixed for 24 h at room temperature in a cacodylate-buffered combined fixative of 1.6% formaldehyde and 2.5% glutaraldehyde. Following three washes in 0.1 M cacodylate buffer (pH 7.42 and mOsm 190), samples were post-fixed in 1% osmium tetroxide for 1 h, dehydrated in graded ethanol and embedded in epoxy resin. Semithin sections, 1 micron thick, were differentiated with basic fuchsin, methylene blue and azure II (Humphrey and Pittman, 1974) and observed by light microscopy. Ultrathin sections, 100 nm thick, were counterstained with uranyl acetate and lead citrate for study by transmission electron microscopy.

RESULTS

Light and electron microscopic analysis demonstrated that in both models the basal cell of the stratum germinativum was selectively affected. The HD-HSE study revealed that basal cell changes began 3 to 6 h following HD exposure (Figs. 1*a-c* and 2*a-d*). These early changes included an apparent acantholysis of some basal cells with widening of intercellular spaces, a disabling of desmosomal attachments, hydropic cytoplasmic changes, nuclear condensations with perinuclear blebbing, and a rearrangement of cytoplasmic tonofilaments to a paranuclear position. At 12 to 24 h, in both the HD-HSE and HD-HGP models basal cell cytopathology progressed to include extensive cytoplasmic vacuolization, swollen endoplasmic reticulum, organelle electron opacities, nuclear pyknosis and cellular necrosis which now involved supra basal cell layers as well.

At the basement membrane zone, the HD-HGP consis-

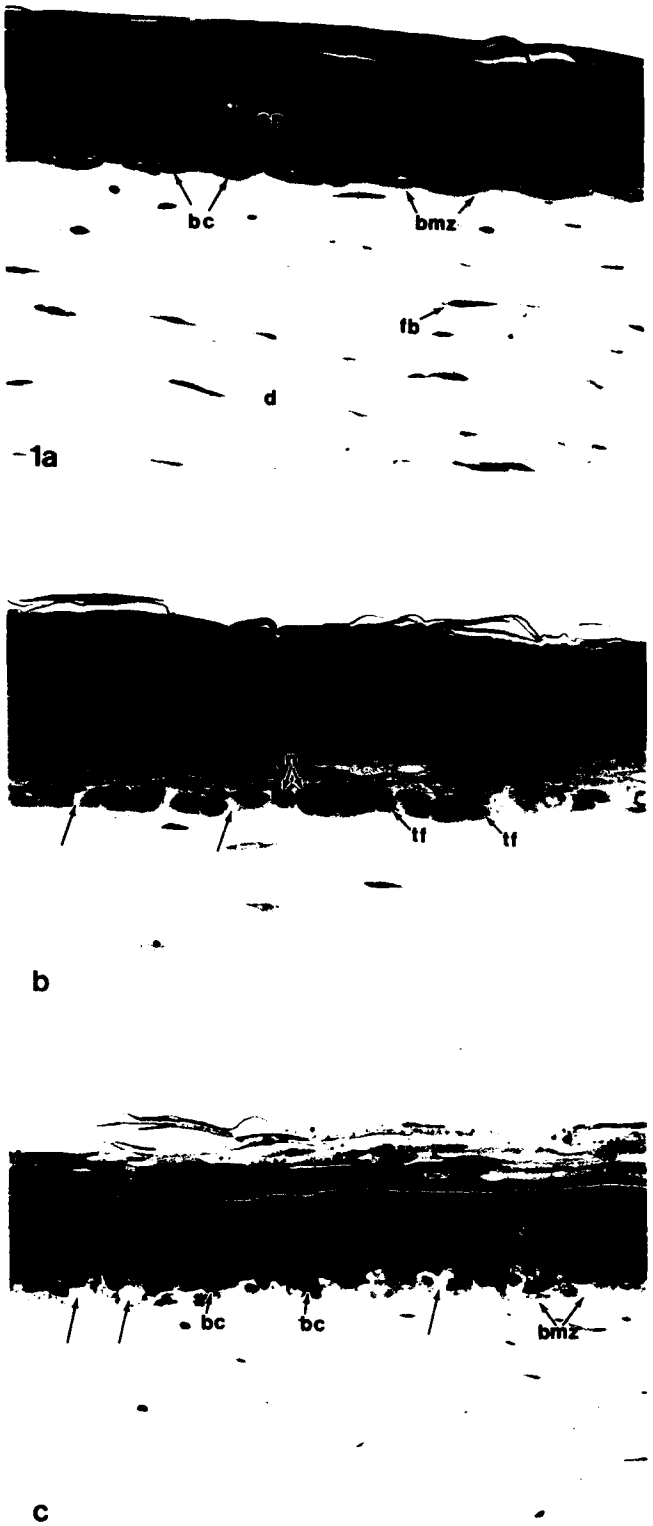

FIGURE 1*a-c* Light microscopy of HD-HSE. (*a*) Control with epidermis (ep) and dermis (d) separated by what appears to be a basement membrane (bmz); basal cells (bc); fibroblast (fb). (*b*) Three hours after HD exposure basal cells undergo nuclear and cytoplasmic changes with loss of attachment to neighboring cells, widening of intercellular spaces (arrows) and perinuclear orientation of tonofilaments (tf); pyknotic basal cell nuclei (n). (*c*) At 6 h basal cells (bc) undergo nuclear and hydropic cytoplasmic changes with fragmentation and loss of cells (arrows). Basement membrane zone (bmz) is thickened. × 250.

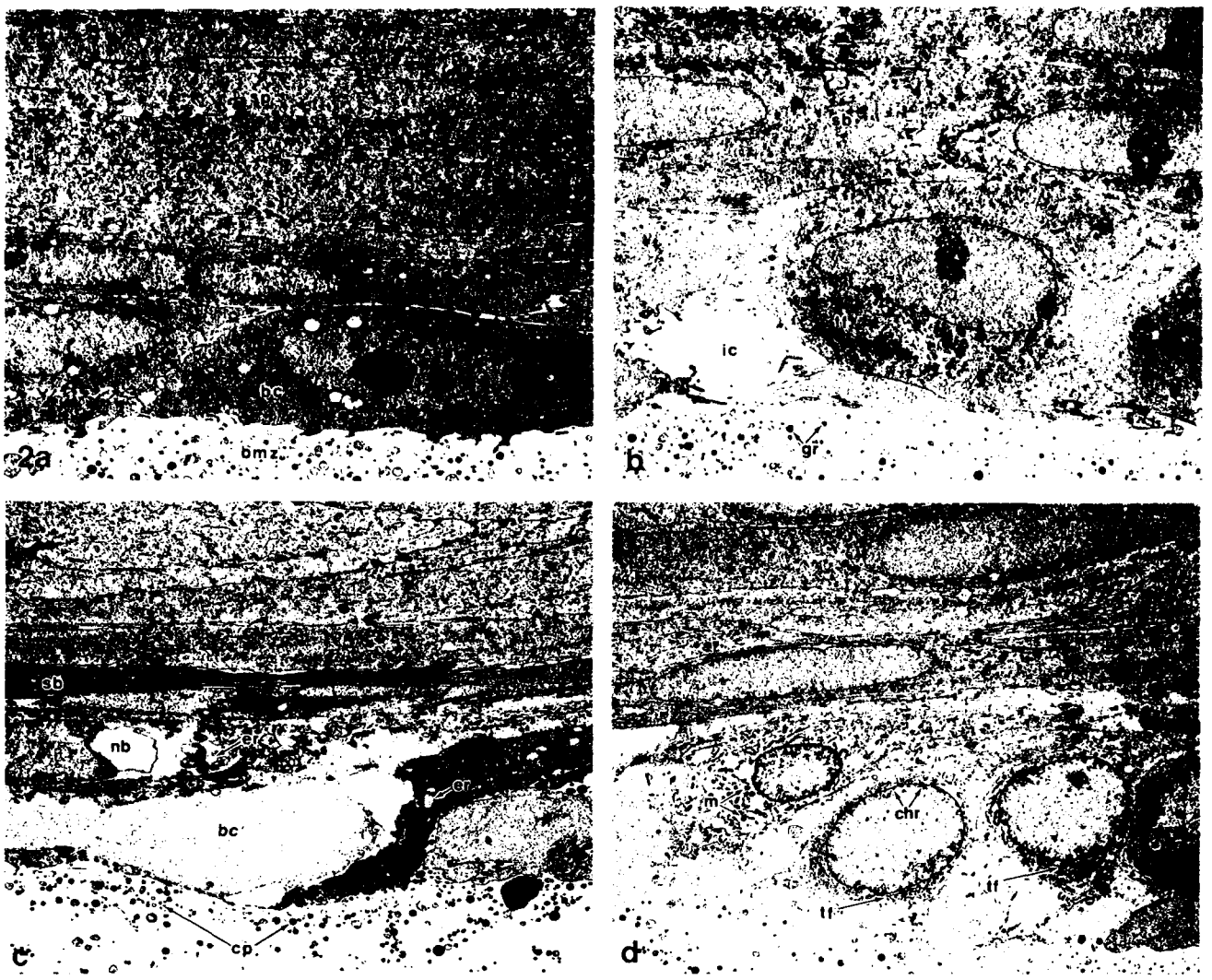

FIGURE 2*a-d*. Electron microscopy of HD-HSE. (*a*) Control HSE at dermal-epidermal junction with absence of structural components of a true basement membrane: basal cell (bc); cellular products in basement membrane zone (bmz); spinosal cell (sp). (*b*) Three hours after HD. Basal cell with tonofibrils in a perinuclear orientation (tf); widened intercellular spaces (ic); supra basal cell (sb); granules (gr). (*c*) At six hours basal cells with perinuclear bleb (nb); swollen endoplasmic reticulum (er); necrotic basal cell (bc); electron dense supra basal cell (sb); cellular particulates (cp). (*d*) Semiadjacent basal cell area at 6 h with margination of basal cell nuclear chromatin (chr); mitochondrial pyknosis (m); perinuclear tonofilaments (tf). (*a-c*) × 3,400, (*d*) × 2,850.

tently generated characteristic microblisters at the dermal-epidermal junction at 12-24 h (Figs. 3*a-c* and 4*a-c*). The cavity, infiltrated with neutrophils, cellular debris and fibers, appeared within the lamina lucida and was formed as a consequence of basal cell pathology and perhaps as a result of the disabling of anchoring filaments of basal cell hemidesmosomes.

The microblister was bound by necrotic basal and epidermal cells at the roof and by the basal lamina of the basement membrane at the floor. However, the HSE with its absence of a morphologically distinguishable basement membrane did not exhibit dermal-epidermal microblisters at any time period. Instead cellular fragments and debris accumulated in the area of the lamina lucida which appeared to widen this space and thicken the basement membrane zone. Ultimately this led to complete separation of epidermis from dermis beginning at the later time periods.

In the course of this study and an earlier study (Petrali *et al.*, 1991) it was observed that skin structures normally present *in vivo* were absent or incomplete in all HSE samples. Absent were hemidesmosomes, a true basement membrane, anchoring filaments and anchoring fibrils. Most desmosomes were morphologically complete; how-

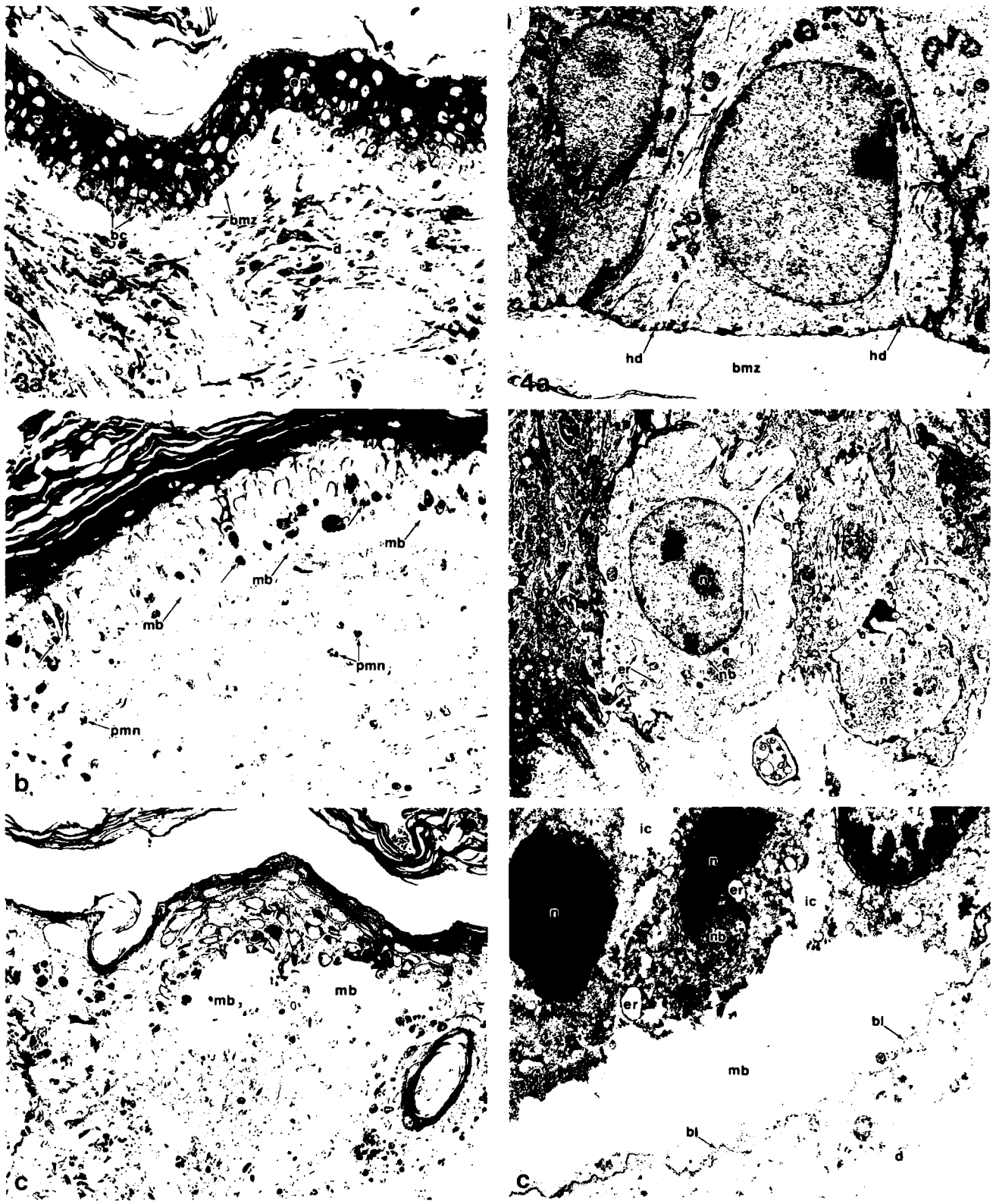

FIGURE 3*a-c* Light microscopy of HD-HGP. (*a*) Control skin epidermis (ep); dermis (d); basement membrane zone (bmz); basal cells of stratum germinativum (bc). (*b*) Twelve hours after HD. Formation of microblisters at the dermal epidermal junction (mb), pyknotic nuclei of basal cells (arrows); polymorphonuclear leukocytes (pmn). (*c*) Twenty four hours following HD. Microblisters coalescing (mb). × 220.

FIGURE 4*a-c* Electron microscopy of HD-HGP. (*a*) Control skin basal cell (bc); tonofilaments (tf); hemidesmosomes (hd); basement membrane zone (bmz). (*b*) Twelve hours after HD. Basal cell nucleus (n); rudimentary nuclear bleb (nb); dilated rough endoplasmic reticulum (er); necrotic basal cell (nc). (*c*) Twenty four hours after HD. Cavity of microblister (mb); basal lamina (bl); pyknotic basal cell nuclei (n); nuclear bleb (nb); exaggerated intercellular spaces (ic); swollen endoplasmic reticulum (er); dermis (d). (*a*) × 5,700, (*b*) × 3,400, (*c*) × 8,550.

ever, some appeared not to have intercellular electron dense plaques typically found at the point of desmosomal attachment.

DISCUSSION

Epithelial basal cell HD-induced cytopathology observed here and those previously reported for other animal models and human cell models in culture were generally similar. Nuclear and cytoplasmic changes lead progressively to basal cell swelling, pyknosis, fragmentation and cell death. Specifically the HSE basal cell pathology was identical to that of other models except for an early widening of intercellular spaces, rearrangement of cytoplasmic tonofilaments and an apparent acantholytic response of some basal cells. This may be related to the observed incomplete morphologic integrity of desmosomes and absence of other epithelial structural components which include hemidesmosomes, and a basement membrane all of which may signal weakened attachments of basal cells to their assigned epidermal strata. The easily recognized perinuclear bleb or paranuclear vacuole by light and electron microscopy was a cellular feature of HD toxicity here as it was in all model systems studied and continues to be useful in identifying those cells affected (Moore *et al.*, 1986; Petrali *et al.*, 1990).

In the HD-HSE system, basement membrane zone effects differed from those observed with *in vivo* animal skin. Typical microblisters did not form at the dermal-epidermal junction. Although the basement membrane components, laminin and type IV collagen, have been immunocytochemically localized to HSE basement membrane zones (Parenteau *et al.*, 1990) in the HSE used for our study the lamina densa and lamina lucida of the dermal-epidermal junction were not distinguishable as morphological entities nor were hemidesmosomes, anchoring filaments and anchoring fibrils. There were instead randomly dispersed unorganized incomplete collagen fibers in close association with neighboring fibroblasts, along with cellular products and granules which collected throughout this area. Following HD toxicity, increased amounts of epithelial cellular products, cellular fragments and cellular debris accumulated at these sites which appeared to widen the space usually assigned to a true lamina lucida. This accumulation early in the toxicity resulted in the formation of a scalloped cleft at the dermal-epidermal junction that separated epidermis from dermis at later time periods.

Morphological correlates of HD toxicity have been compared in a five model pedigree: the human skin grafted athymic nude mouse, the hairless guinea pig, human lymphocytes and keratinocytes in culture, and now an *in vitro* human skin equivalent. In the case of *in vivo* studies, targeting of skin basal cells and effects at the dermal epidermal junction have been morphologically characterized. However, primary or secondary effects on specific morpho-biochemical components of the basement membrane zone as well as effects on basal cell extracellular matrices are yet to be realized. Among these extracellular domains are skin structural proteins which in the case of some bullous diseases are known to be altered to specific antisera (Fine, 1987). In a recent immunohistochemical study of mustard gas skin lesion, laminin and bullous pemphigoid antigen were shown to be altered to recognition by specific antisera following exposure to HD. This reported loss of specific immunoreactivity of structural proteins suggests that extracellular matrices of the basement membrane zone are affected during the development of HD-induced skin pathology and may be contributory to the formation of microblisters (Petrali *et al.*, 1992).

Time course HD studies using cultured human monotypic cells have added useful subcellular information on temporal effects on nuclei and cytoplasmic organelles. Condensation of chromatin, nuclear membrane blebbing, swelling of endoplasmic reticulum and plasmalemmal changes have provided morphological cues of expected and predicted biochemical lesions associated with HD toxicity. A suggested HD-biochemical lesion cascade involves the activation of poly(ADP-ribose)polymerase, a lowering of cellular NAD concentrations, inhibition of glycolysis, and activation of the hexose monophosphate shunt which may stimulate release of cellular proteases leading to observed cytopathologic changes (Papirmeister *et al.*, 1985, 1991).

In the present study, an important advantage of using an organotypic HSE system was that it responded to HD toxicity without the additive, subtractive or otherwise modulating effects of hemal-borne inflammatory chemical mediators. As such, it afforded opportunity to measure morphological cellular responses to HD with the knowledge that the response was mediated largely by dose of HD, by virtue of the cytoarchitectural design and by perhaps endogenous cellular chemical mediators now being identified in HSE systems (Parenteau *et al.*, 1990). In addition, it provided replicate HD study of an *in vitro* stratified cellular system as opposed to isolated monolayered monotypic cells in culture, which typically present a persistent but surely an acclimatized morphology as they exist and respond in a completely liquid environment. Detracting however from the complete morphological usefulness of the HSE as an organotypic skin equivalent HD model was the lack of important skin structures that may serve to play a role in the *in vivo* pathogenesis of HD toxicity. Their absence may account for the observed disparate responses of the HD-HSE model when compared to the HD-HGP model in this study.

REFERENCES

Bell E., Gay R., Swiderek M., Class T., Kemp P Green G., Haimes H. and Bilbo P., 1989. Use of fabricated living tissue and organ equivalents as defined higher order systems for the study of pharmacologic response to test substances. NATO Advanced Research Workshop, Pharmaceutical Application of Cell & Tissue Culture to Drug Transport, Bandol, France, 4-9 September 1989.

Fine J., 1987. Altered skin basement membrane antigenicity in epidermolysis bullosa. *Curr. Probl. Dermatol.*, **17**, 111-126.

Humphrey C.D. and Pittman F.E., 1974. A simple methylene blue, azure II and basic fuchsin stain for epoxy embedded tissue sections. *Stain. Technol.*, **49**, 9-14.

Mershon M.M., Mitcheltree L.W., Petrali J.P., Braue E.H. and Wade J.V., 1990. Hairless guinea pig bioassay models for vesicant vapor exposure. *Fundam. Appl. Toxicol.*, **15**, 622-630.

Moore K.G., Schofield B.H., Higuchi K., Kajiki A., Au K.W., Pula P.J., Bassett D.B. and Dannenberg A.M., 1986. Two sensitive in vitro monitors of chemical toxicity to human and animal skin (in short-term organ culture). I. Paranuclear vacuolization in glycol methacrylate tissue sections. II. Interference with ^{14}C-leucine incorporation. *J. Toxicol.-Cut. Ocular Toxicol.*, **5**, 285-302.

Papirmeister B., Gross C.L., Petrali J.P. and Hixson C.J., 1984. Pathology produced by sulfur mustard in human skin grafts on athymic nude mice. *J. Toxicol.-Cut. Ocular Toxicol.*, **3** (4), 371-408.

Papirmeister B., Gross C., Meier H., Petrali J. and Johnson J., 1985. Molecular basis for mustard-induced vesication. *Fundam. Appl. Toxicol.*, **5**, S134-S149.

Papirmeister B., Feister A.J., Robinson S.I. and Ford R.D., 1991. 'Medical Defense Against Mustard Gas: Toxic Mechanisms and Pharmacological Implications'. CRC Press, Boca Raton, Florida.

Parenteau N., Bilbo P., Nolte C. and Gay R., 1990. How well does the epidermis differentiate in vitro? UCLA Symposium on Tissue Engineering, Keystone, Colorado, 6-12 April 1990.

Petrali J.P., Oglesby S.B. and Mills K.R., 1990. Ultrastructural correlates of sulfur mustard toxicity. *J. Toxicol.-Cut. Ocular Toxicol.*, **9** (3), 193-214.

Petrali J.P., Oglesby S.B. and Justus T.A., 1991. Morphologic effects of sulfur mustard on a human skin equivalent. *J. Toxicol.-Cut. Ocular Toxicol.*, **10** (4), 315-324.

Petrali J.P., Oglesby S.B., Hamilton T.A. and Mills K.R., 1992. Ultrastructural pathology and immunohistochemistry of mustard gas lesion. Proceedings of the Electron Microscopy Society of America, Part 1, pp. 826-827.